doi:10.3772/j.issn.1006-6748.2017.03.002

Quantitative analysis of the performance of vector tracking algorithms①

Wang Qian (王 前)②*, Cui Xiaowei**, Liu Jing**, Zhao Sihao**
(*Beijing Satellite Navigation Center, Beijing 100094, P. R. China)
(**Department of Electronic Engineering, Tsinghua University, Beijing 100084, P. R. China)

Abstract

Vector tracking changes the classical structure of receivers. Combining signal tracking and navigation solution, vector tracking can realize powerful processing capabilities by the fusion technique of receiving channel and feedback correction. In this paper, we try to break through the complicated details of numerical analysis, consider the overall influencing factors of the residual in observed data, and use the intrinsic link between a conventional receiver and a vector receiver. A simple method for performance analysis of the vector tracking algorithm is proposed. Kalman filter has the same steady performance with the classic digital lock loop through the analysis of the relation between gain and band width. The theoretical analysis by the least squares model shows that the reduction of range error is the basis for the superior performance realized by vector tracking. Thus, the bounds of its performance enhancement under weak signal and highly dynamic conditions can be deduced. Simulation results verify the effectiveness of the analysis presented here.

Key words: vector tracking, dynamic stress noise, loop band width, pseudo-range error

0 Introduction

Satellite navigation systems can provide precise real-time positioning, velocity measurements, and timing services in all weather conditions and at any location. With continuous expansion and improvement of human production and living standards, the requirements of satellite navigation terminals have increased. Traditional receiving terminals cannot perform optimally in highly dynamic and weak signal conditions, which is a major limit on satellite navigation applications. A series of solutions for improving satellite navigation terminal performance have appeared, including inertial navigation assistance, satellite power boosting, and vector tracking.

Among all of the aforementioned solutions, only "vector tracking" focuses on improving receiver performance without the help of an auxiliary external system, which has made vector tracking an active and growing area of research. The basic idea of vector tracking[1] is to combine channel tracking and navigational information from all of the received channels using an extended Kalman filter. The position results are obtained while simultaneously using measured values as a feedback signal for the local oscillator in order to maintain stable satellite signal tracking.

Compared with a traditional scalar-loop structure, a vector-loop receiver can indeed exhibit superior performance. In particular, a vector-loop receiver can achieve stable tracking under highly dynamic and weak signal conditions. The advantage of vector-loop channel fusion effectively reduces the measurement error, thereby enhancing the carrier-to-noise ratio and sensitivity of the receiver. In dynamic environments, vector tracking algorithms can use vector decomposition to track dynamic signals in the correct direction by using characteristics of the motion to offset the dynamic stress in a strong dynamic direction, and reduce ineffective setting in a weak dynamic direction.

Many publications have presented detailed analyses that quantify the advantages of vector loop performance. Refs[2] and [3] presented comparative analyses of vector and scalar loop receiver performance under different scenarios. Ref. [3] emphasized the superiority of vector loops under the condition of losing and recapturing lock. Ref. [4] described the tracking performance exhibited by a vector loop under the condition of ionospheric scintillation. Ref. [5] compared and analyzed the tracking performance of scalar and vector loops based on Kalman filtering under the condition of

① Supported by the National Natural Science Foundation of China (No. 41474027) and the National Defense Basic Science Project (JCKY2016110B004).
② To whom correspondence should be addressed. E-mail: wqaloha@139.com
Received on June 8, 2016

lower signal to noise ratio. All of the aforementioned documents emphasize the tracking advantages of vector loops in various harsh environments, however, systematic and in-depth analyses of the performance of vector tracking algorithms are limited.

Ref. [6] provided a more detailed analysis on the performance advantages of vector loops. The general idea is as follows: the thermal noise tracking is determined by the matrix of the mean square deviation of the error, P_{ss}^{+}. By using the Kalman filter equations, P_{ss}^{+} can be calculated. When the Kalman filter reaches steady state it fits the Riccati equation, but the equation has no analytical solution in mathematics, i. e., such analysis has only theoretical significance and cannot provide practical help in engineering applications. Thus, the thermal noise effect of the loop can only be estimated through numerical simulation if the drive noise variance is fixed. The error analysis in the presence of dynamic stress is similar, with the main difference being the addition of an input controlling variable vector in the system equations.

Based on the aforementioned research work, this article focuses on the physical factors that influence vector tracking algorithm performance, and points out the role of the Kalman filter in the algorithm. Starting from a bandwidth analysis, an in-depth discussion on how vector tracking achieves excellent performance with highly dynamic and weak signals is presented. A theoretical analysis that quantifies the enhancement range of vector tracing performance for engineering applications is proposed and verified by simulation.

1 Model description

1.1 Signal model

The downlink signal in satellite navigation system is modulated by pseudo code and carrier wave. The signal is input to the base band after frequency conversion through RF module, which can be expressed by

$$x(t) = \sum_{i=1}^{N} a_i S_i(t - \tau_i) \exp\{j2\pi f_{d,i} t + j\varphi_i\} + n(t) \quad (1)$$

where, t is the receiving moment, N is the number of visible satellites, and a_i, τ_i, φ_i and $f_{d,i}$ are the amplitude, the phase delay, the carrier phase, and the Doppler frequency shift of signal i, respectively. $S_i(t - \tau_i)$ is the modulation spreading code for the corresponding signal, and $n(t)$ is white Gaussian noise. The process of tracking in the receiver is used to obtain the aforementioned signal parameters from the noise signal. A scalar loop obtains the parameters of a single branch through an independent DLL (delay locked loop) /FLL (frequency locked loop) minor feedback loop, while a vector loop obtains the parameters of all of the branches simultaneously through a VDLL/VFLL major feedback loop.

1.2 Vector loop structure model

The model of a vector loop is shown in Fig. 1, and the core is based on discrete time state recursion. In the initial stage of system operation, estimates of the necessary signal parameter information of position and velocity are obtained via a scalar loop as mentioned in Section 1.1. After this initial operation, the scalar loop connection between the discriminator and the local reference oscillator should be disconnected. The discriminator outputs the predicted error vector of the observed value and, by processing this data with a Kalman filter, the vectors of displacement and velocity can

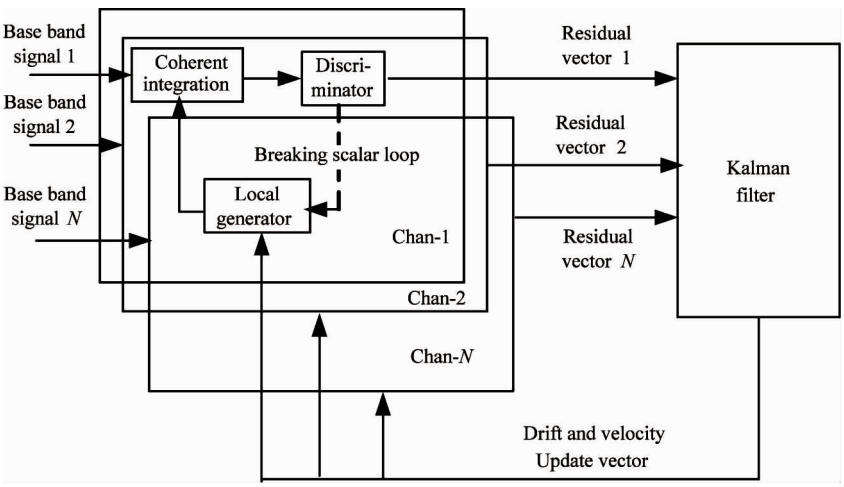

Fig. 1 The model of a vector loop

be updated. After radial projection in the direction of the satellite, the predicted code phase/frequency and carrier frequency can be obtained in order to drive the local reference oscillator to recover the pseudo code and carrier information. Thus, a complete signal vector tracking process is realized.

During continuous operation of the vector loop, updates of the Kalman gain are mainly based on the following recursion formula:

$$\begin{aligned} \boldsymbol{P}_k^- &= \boldsymbol{A}_k \boldsymbol{P}_{k-1}^+ \boldsymbol{A}_k^{\mathrm{T}} + \boldsymbol{Q}_k \\ \boldsymbol{K}_k &= \boldsymbol{P}_k^- \boldsymbol{H}_k^{\mathrm{T}} [\boldsymbol{H}_k \boldsymbol{P}_k^- \boldsymbol{H}_k^{\mathrm{T}} + \boldsymbol{R}_k]^{-1} \\ \boldsymbol{P}_k^+ &= (\boldsymbol{I} - \boldsymbol{K}_k \boldsymbol{H}_k) \boldsymbol{P}_k^- \end{aligned} \tag{2}$$

where $\boldsymbol{A}_k$ is the state conversion matrix, $\boldsymbol{H}_k$ is the measurement matrix, $\boldsymbol{P}_k^-$ is the covariance matrix of the state error of the prior prediction, and $\boldsymbol{P}_k^+$ is the covariance matrix of the adjusted posterior prediction. The process of Kalman filtering is essentially a process of constant gain adjustment, which can also be described as a self-adapting change in the filter bandwidth[7,8].

1.3 Influence factor analysis

As shown in Fig. 1, the Kalman filter is the core of the vector loop, and its parameters directly influence the performance of the vector tracking algorithm. The state variables of the filter are signal synchronization parameters such as power, code phase and carrier Doppler. In the corresponding mode the measure variables are the surplus estimations of the above parameters derived from the descriminators. In general, Kalman filtering consists of two processing procedures: "prediction" and "correction", where the state noise and measurement noise should be used, respectively. The covariance matrix of the state noise is composed of signal power noise and carrier Doppler noise. Note that carrier Doppler noise depends on the state of satellite motion, receiver motion, and the clock drift of user's equipment. The covariance matrix of measurement noise consists of the residual code phase delay, the residual Doppler shift, and the discriminator error variance for the residual signal power. The discriminator commonly adopts the non-coherent power method, for which the expression of discriminator error variance[9] is

$$\sigma_{\sigma\tau_i}^2 = \frac{1}{f_{code}^2} \frac{d}{4TC_i/N_0} \left(1 + \frac{2}{(2-d)TC_i/N_0}\right) \tag{3}$$

$$\sigma_{\sigma f_{d,i}}^2 = \frac{2}{\pi^2 T^3 C_i/N_0} \left(1 + \frac{2}{TC_i/N_0}\right) \tag{4}$$

$$\sigma_{\delta a_i^2}^2 = 2a_i^2 \frac{N_0}{T} \left(1 + \frac{1}{TC_i/N_0}\right) \tag{5}$$

where, d is the spacing of the correlators, T is the coherent integration time, C_i/N_0 is the carrier to noise ratio of i_{th} channel, $\sigma_{\sigma\tau_i}^2$, $\sigma_{\sigma f_{d,i}}^2$ and $\sigma_{\delta a_i^2}^2$ are the discriminator error variances of the residual code phase delay, the residual Doppler shift, and the residual signal power, respectively. By setting the parameters for the state noise and measurement noise, the sensitivity of the vector loop to these influence factors can be quantified, which includes the quality of the received signal, the dynamic characteristics, the coherent integration time, the crystal oscillator stability of the user's equipment, etc.

2 Theoretical analysis

2.1 Thermal noise analysis

In order to facilitate the thermal noise analyses, one can assume that the quality of the received signal is the same for different channels. The pseudo range measurement model of the scalar loop is shown in Eq. (6). As each channel is independent, the transfer matrix is set as a unit array, where $\boldsymbol{\delta\tilde{\rho}}$ is the change of the pseudo range, and $\boldsymbol{\delta\rho}$ is the unknown change of the pseudo range which needs to be solved for.

$$\begin{bmatrix} \delta\tilde{\rho}_1 \\ \delta\tilde{\rho}_2 \\ \vdots \\ \delta\tilde{\rho}_m \end{bmatrix} = \begin{bmatrix} 1 & 0 & 0 & \cdots & 0 \\ 0 & 1 & 0 & \cdots & 0 \\ \tilde{\rho} & & & & \vdots \\ 0 & \cdots & \cdots & \cdots & 1 \end{bmatrix} \cdot \begin{bmatrix} \delta\rho_1 \\ \delta\rho_2 \\ \vdots \\ \delta\rho_m \end{bmatrix} + \begin{bmatrix} v_1 \\ v_2 \\ \vdots \\ v_m \end{bmatrix} \tag{6}$$

$$\begin{aligned} \boldsymbol{\Delta\tilde{\rho}} &= \boldsymbol{I}_{m\times m} \cdot \boldsymbol{\Delta\rho} + \boldsymbol{V} \\ E\{\boldsymbol{V}\boldsymbol{V}^{\mathrm{T}}\} &= \sigma_v^2 \cdot \boldsymbol{I}_{m\times m} = \boldsymbol{R}_v \end{aligned} \tag{7}$$

Using the least squares method, the pseudo range estimation is obtained: $\boldsymbol{\Delta\hat{\rho}} = (\boldsymbol{I}_{m\times m} \cdot \boldsymbol{R}_v^{-1} \cdot \boldsymbol{I}_{m\times m})^{-1} \cdot \boldsymbol{I}_{m\times m}^{\mathrm{T}} \cdot \boldsymbol{R}^{-1} \cdot \boldsymbol{\Delta\tilde{\rho}}$, so the measurement error variance of the scalar loop is obtained: $E\{\boldsymbol{\Delta\hat{\rho}}\boldsymbol{\Delta\hat{\rho}}^{\mathrm{T}}\} = (\boldsymbol{I}_{m\times m} \cdot \boldsymbol{R}_v^{-1} \cdot \boldsymbol{I}_{m\times m})^{-1} = \sigma_v^2 \cdot \boldsymbol{I}_{m\times m}$.

According to the principle of the vector loop, the displacement vector can be transformed into a pseudo range variation only by radial projection in the direction of the carrier and satellite.

$$\begin{bmatrix} \delta\tilde{\rho}_1 \\ \delta\tilde{\rho}_2 \\ \vdots \\ \delta\tilde{\rho}_m \end{bmatrix} = \begin{bmatrix} a_{x,1} & a_{y,1} & a_{z,1} & 1 \\ \vdots & \vdots & \vdots & \vdots \\ a_{x,m} & a_{y,m} & a_{z,m} & 1 \end{bmatrix} \cdot \begin{bmatrix} \delta x \\ \delta y \\ \delta z \\ c\delta t \end{bmatrix} + \begin{bmatrix} v_1 \\ v_2 \\ \vdots \\ v_m \end{bmatrix}$$

$$\boldsymbol{\Delta\tilde{\rho}} = \boldsymbol{H}_{m\times 4} \cdot \boldsymbol{\Delta X} + \boldsymbol{V} \tag{8}$$

Similarly, according to the least square method, equation

$$\boldsymbol{\Delta X} = (\boldsymbol{H}_{m\times 4}^{\mathrm{T}} \cdot \boldsymbol{R}_v^{-1} \cdot \boldsymbol{H}_{m\times 4})^{-1} \cdot \boldsymbol{H}_{m\times 4}^{T} \cdot \boldsymbol{R}_v^{-1} \cdot \boldsymbol{\Delta\tilde{\rho}} \tag{9}$$

can be solved as:

$$\begin{aligned} E\{\boldsymbol{\Delta X}\boldsymbol{\Delta X}^{\mathrm{T}}\} &= (\boldsymbol{H}_{m\times 4}^{\mathrm{T}} \cdot \boldsymbol{R}_v^{-1} \cdot \boldsymbol{H}_{m\times 4})^{-1} \\ &= \sigma_v^2 \cdot (\boldsymbol{H}_{m\times 4}^{\mathrm{T}} \cdot \boldsymbol{H}_{m\times 4})^{-1} \end{aligned} \tag{10}$$

The estimated variation of a pseudo range can then be expressed as

$$\Delta\hat{\rho} = H_{m\times 4} \cdot \Delta X \tag{11}$$

And the error variance of vector loop equals to:

$$E\{\Delta\hat{\rho}\Delta\hat{\rho}^{\mathrm{T}}\} = \sigma_v^2 \cdot H_{m\times 4} \cdot (H_{m\times 4}^{\mathrm{T}} \cdot H_{m\times 4})^{-1} \cdot H_{m\times 4}^{\mathrm{T}} = \sigma_v^2 \cdot W_{m\times m} \tag{12}$$

Under the condition that the weight of each channel is identical, the variance of the pseudo range noise is reduced from σ_v^2 in the scalar loop to $\frac{4}{m}\sigma_v^2$ in the vector loop. The noise variance reduction in the pseudo range means the signal quality is improved (i. e., an improvement in the carrier to noise ratio), which also demonstrates the ability of the vector loop to deal with weak signals. The parameters of the loop are set as follows: the coherent integration time is 2ms and 20ms, the loop bandwidth is 2Hz, and the carrier to noise ratio of the received signal is 18dB · Hz for each scalar loop channel. Table 1 lists the effective improvement in the carrier to noise ratio of the signal after the feedback of vector loop tracking for different numbers of channels. As shown in the table, when the number of channels is increased, the effect of the signal enhancement is more obvious. The amplitude of the integral at 2ms increases from 0.9dB to 2.5dB, and the amplitude of the integral at 20ms increases even more, from 1.1dB to 3.4dB.

Table 1 The processing performance of weak signals by the vector loop

Interval \ Channel number	6	7	8	9	10	11	12	Integration time
1 chip	18.9106	19.2584	19.5605	19.8276	20.0672	20.2844	20.4831	
0.5 chip	18.9234	19.2774	19.5852	19.8578	20.1025	20.3246	20.5279	2ms
0.25 chip	18.9342	19.2912	19.6019	19.8772	20.1244	20.3488	20.5545	
1 chip	19.1107	19.5459	19.9286	20.2709	20.5810	20.8649	21.1267	
0.5 chip	19.1897	19.6571	20.0691	20.4381	20.7729	21.0795	21.3626	20ms
0.25 chip	19.2024	19.6827	20.1062	20.4857	20.8299	21.1451	21.4363	

2.2 Dynamic stress analysis

$$\theta_e = \begin{cases} \alpha \dfrac{d^n R/dt^n}{B^n} (\text{code\_loop}) \\ \alpha \dfrac{d^{n+1} R/dt^{n+1}}{B^n} (\text{frequency\_loop}) \end{cases} \tag{13}$$

The classical expression of dynamic stress error is shown in Eq. (13), where α is the loop bandwidth, B is the empirical coefficient of characteristic frequency conversion, R is the distance between the carrier and the satellite, and n is the loop order. The value of the dynamic stress is mainly related to two factors: 1) the relative dynamic state between the carrier and the satellite, and 2) the characteristic frequency, which is closely related to the loop bandwidth. Because the dynamic stress error generated in the transient response is much larger than that in the steady state response, the loop bandwidth is generally conservative in order to guarantee the signal frequency and phase change caused by the dynamic motion of the loop are rejected.

In Section 2.1, it shows that a vector loop improves the noise performance of the loop, which reduces the requirement of a conservative loop bandwidth. Therefore, the bandwidth can be increased to increase signal tracking performance in the presence of dynamic stress.

Under the premise of the same noise variance, the loop bandwidth of a vector loop can be increased to improve adaptability to the dynamic stress error experienced by the receiving terminals. Fig. 2 shows that the tolerance of the loop bandwidth increases gradually as the carrier to noise ratio increases. Moreover, if the coherent integration time is longer, this advantage is more obvious. When the carrier to noise ratio increases from 18dB · Hz to 20.5dB · Hz, the bandwidth of the 2ms integral increases from 2Hz to 4.5Hz, and the bandwidth of the 20ms integral increases from 2Hz to 6Hz. However, the ability to increase the integration time is always limited by factors such as the message data, dynamic stress, frequency stability of the crystal oscillator in the receiver, etc. Thus, it is not suitable to set the integration time too long. Note that the input of the vector loop still employs the frequency discriminator output of a traditional scalar loop, therefore, the threshold value of the frequency tracking loop can be expressed by

$$3\sigma_w + \theta_e \leqslant \frac{0.25}{T} \tag{14}$$

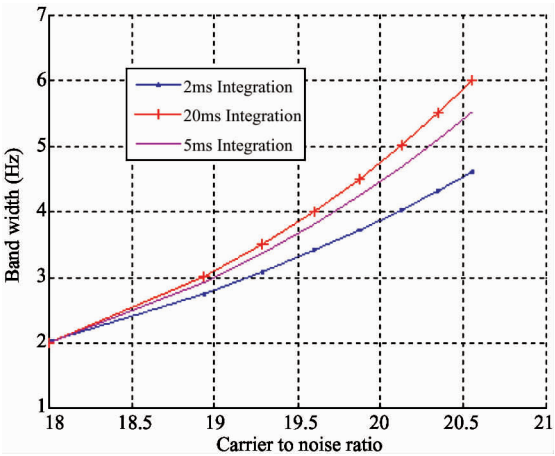

Fig. 2 The bandwidth variation under weak signal conditions

In Eq. (14), σ_w is the root mean square of the frequency error caused by thermal noise, and θ_e is the tracking error caused by the dynamic stress. Under weak signal conditions σ_w is very large, so the margin for dynamic stress is very small, and the effect of the increase in dynamic range is not obvious.

When the carrier to noise ratio is relatively high, the curve in Fig. 3 indicates that the effect of the integration time on performance can be neglected. To summarize, according to Eq. (13) with all other parameters being equal, doubling the bandwidth in a first order loop increases the tolerable dynamic stress by a factor of 2, and doubling the bandwidth in a second order loop increases the tolerable dynamic stress by a factor of 4.

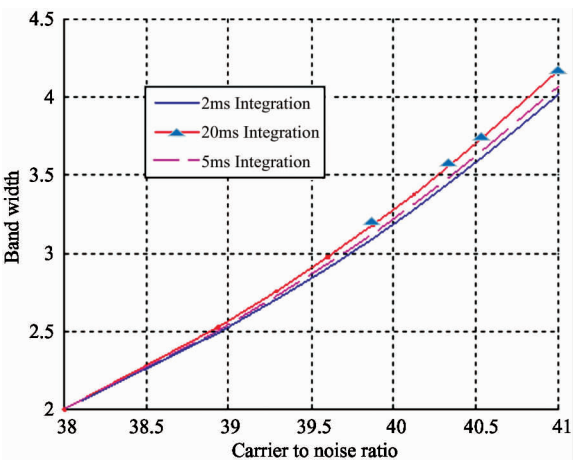

Fig. 3 The bandwidth variation under strong signal conditions

3 Performance Verification

3.1 Simulation environment

In the simulation results presented here, a signal generator produces the multi-channel BPSK navigation signal. The signal intensity in each channel is constant, and C/N_0 is set to 19dB · Hz for a weak signal, and 40dB · Hz for a normal signal. The Nyquist sampling rate is 8.184MHz, and the simulation duration is 400s. The simulated movement is a combination of uniform acceleration and sudden acceleration. The acceleration jumps from 0.5g m/s^2 to −0.5gm/s^2, where the high one is from 6g m/s^2 to −6g m/s^2. Signal setting of simulation is consistent with the presented tracking threshold of VDFLL[10].

The two receivers implemented here use a scalar receiver and a vector VDFLL receiver, respectively. For a fair comparison between the two types of algorithms, both are based on the tracking loop of a Kalman filter and the influence of a changing loop bandwidth on the algorithm performance is neglected. Observation noise parameters are captured directly from the output value of the discriminator, and process noise parameters are fixed under weak signal conditions without the adaptability adjustment that could be obtained from the variation of the dynamic state of the carrier. Although this parameter adjustment is useful for improving the performance, it prevents comparing the two algorithms on the same platform. Under highly dynamic conditions, the bandwidth parameter is adjusted according to the dynamic state while maintaining the same measurement error is desired. The loop integral time is set to 20ms in all cases.

3.2 Weak signal processing analysis

Fig. 4 and Fig. 5 list the code phase delay error, carrier frequency error due to Doppler shifts for different numbers of satellites (6, 8, and 11), respectively under weak signal conditions (19dB · Hz, ±0.5g m/s^2). These conditions provide insight into the processing capability of the VDFLL architecture in a weak signal environment. Fig. 4 and Fig. 5 reveal that with an increasing number of satellites, the code phase error and carrier frequency error are both reduced. When the number

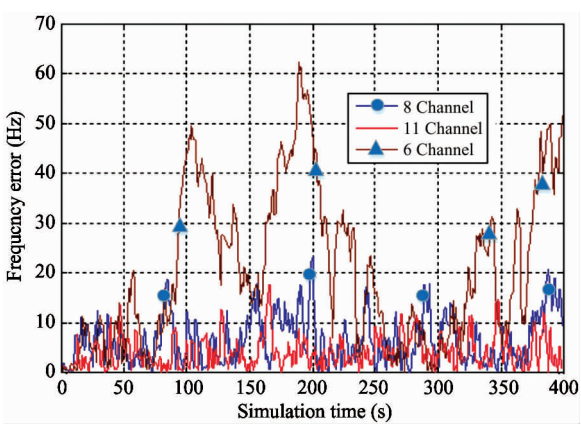

Fig. 4 Frequency error under weak signal conditions

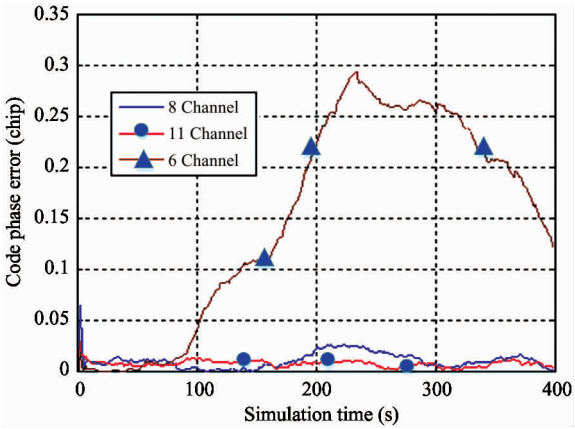

Fig. 5 Code phase error under weak signal conditions

of satellites is 6, FLL and DLL are out of lock, so the error is large. Scalar receivers with same settings can achieve a stable tracking state for the signal parameters of (23dB · Hz, ±0.5g), which is in line with the theoretical analysis presented in Section 2.

3.3 Dynamic stress processing analysis

Fig. 6 and Fig. 7 list the code phase delay error, carrier frequency error due to Doppler shifts, and position error for different numbers of satellites (6, 8, and 11), respectively, under highly dynamic conditions (40dB · Hz, ±6g m/s^2) in order to investigate the processing capability of the VDFLL architecture in a highly dynamic environment. Due to different simulation parameters, the results are not entirely consistent with those obtained in the weak signal environment. Owing to the excellent signal quality, the errors of code phase with different satellite number are not obvious. From Fig. 7, it should be pointed out that the frequency error of channel 6 is between 8 and 12Hz,

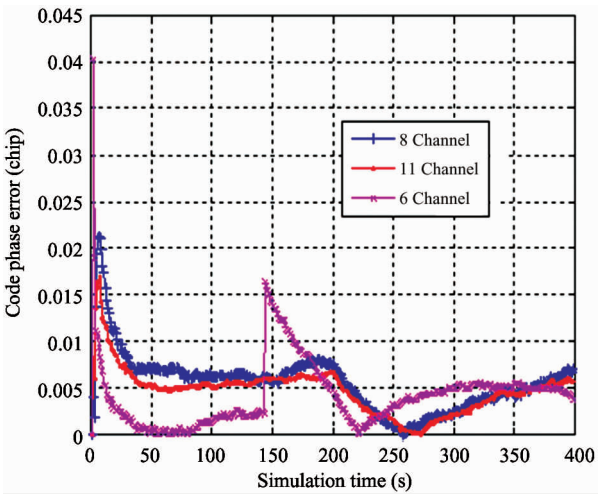

Fig. 6 Code phase error in highly dynamic conditions

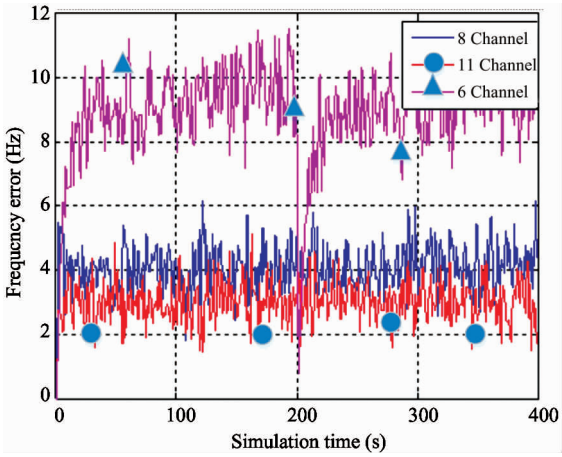

Fig. 7 Frequency error in highly dynamic conditions

which is close to the threshold value of the FLL's tracking bandwidth (12.5Hz). Therefore, it is the loss of lock in the FLL that causes the final positioning failure. In addition to the bandwidth parameters, the other scalar receivers with the same parameter settings reach a stable tracking state for the signal parameters of (40dB · Hz, ±3g m/s^2), which is in good agreement with the theoretical analysis presented in Section 2.

3.4 Validation with actual data

In order to validate the performance, an actual real-time data is used by RF signal recording and playback apparatus[11]. The trajectory of the vehicle on the highway with the velocity of 90km/h is shown as Fig. 8. The C/N_0 of GPS collected satellite signal is 44dB · Hz.

Fig. 8 Trajectory of the vehicle on the highway

In this condition, the measure errors of VDLL and VFLL with the vector loop are 0.0021 chip and 0.45Hz, while those with the scalar loop are 0.0032 chip and 3.8Hz. This experiment shows the advantage of VDLL/VFLL in signal tracking compared with DLL/FLL in the regular scene.

4 Conclusion

The vector tracking architecture in global navigation satellite system (GNSS) receivers has the advantage of increased performance through multi-channel integration processing, but it also has disadvantages including a complex structure and the need to perform a large number of calculations. Thus, analyzing its performance is also a problem in industry settings. In this paper, transformation between vector tracking and scalar tracking is used to determine the influence and constraints of integration time, loop bandwidth, thermal noise, dynamic stress, and other factors that affect receiver performance. The vector loop can reduce the observation error and improve performance through accurate feedback obtained by multi-channel fusion technology. Under equivalent conditions, the vector receiver exhibits a gain that is 3dB higher, or endures 2 ~ 4 times the dynamic stress, when compared with a scalar receiver.

Reference

[1] Sennott J W. A flexible GPS software development system and timing analyzer for present and future microprocessors. *Navigation*, 1984, 31(2): 84-95

[2] Lashley M, Bevly D M, Hung J Y. A valid comparison of vector and scalar tracking loops. In: Proceedings of the IEEE/ION Position Location and Navigation Symposium (PLANS), Indian Wells, USA, 2010. 464-474

[3] Kanwal N, Hurskainen H, Nurmi J. Vector tracking loop design for degraded signal environment. In: Proceedings of International Conference on Ubiquitous Positioning Indoor Navigation and Location Based Service, Kirk konummi, Finland, 2010. 1-4

[4] Xia J, Yue F Z, Wang P P, et al. Robust GNSS signal tracking algorithm based on vector tracking loop under ionospheric scintillation conditions. In: Proceedings of the 12th International Conference on Signal Processing, Hangzhou, China, 2014. 2385-2389

[5] Zhao S H, Lu M Q, Feng Z M. GNSS vector lock loop based on adaptive Kalman filter. *Journal of Harbin Institute of technology*, 2012, 44(7): 139-143 (In Chinese)

[6] Lashley M, Bevly D M, Hung J Y. Performance analysis of vector tracking algorithms for weak GPS signals in high dynamics. *IEEE Journal of Selected Topics in Signal Processing Selected*, 2009, 3(4): 661-673

[9] Van Dierendonck A J, Fenton P, Ford T. Theory and performance of narrow correlator spacing in a GPS receiver. *Navigation*, 1992, 39(3): 265-284

[7] Qian Y, Cui X W, Lu M Q, et al. Steady-state performance of Kalman filter for DPLL. *Tsinghua Science and Technology*, 2009, 14(4): 470-473 (In Chinese)

[8] Wang Q, Hu C B. Kalman filter signal tracking based on relatively fixed-gain. *Chinese High Technology Letters*, 2015, 25(1): 17-23 (In Chinese)

[10] Liu J, Cui X W, Lu M Q, et al. Vector tracking loops in GNSS receivers for dynamic weak signals. *Journal of Systems Engineering and Electronics*, 2013, 24(3): 349-364

[11] Xian D Y, Fan P R, Wu H L. Test system for BDS user terminal based on RF replay apparatus. In: Proceedings of the 7th China Satellite Navigation Conference, Changsha, China, 2016, 5: 413-422

Wang Qian, born in 1978. He received his Ph. D degree in Computer Science Department of Beihang University. His research interests include the design of algorithms for signal tracking, integrated navigation and precision positioning.